

Lukassen et al.

TGFBI<sup>R124H</sup> mouse proteome**Dataset Brief****Protein analysis of the TGFBI<sup>R124H</sup> mouse model gives insight into phenotype development of granular corneal dystrophy**

Marie V. Lukassen<sup>1,2</sup>, Ebbe T. Poulsen<sup>1</sup>, Jack Donaghy<sup>3</sup>, Emilie H. Mogensen<sup>1</sup>, Kathleen A. Christie<sup>3</sup>, Hila Roshanravan<sup>4</sup>, Larry DeDioniso<sup>4</sup>, M. Andrew Nesbit<sup>3</sup>, Tara Moore<sup>3,4\*</sup>, Jan J. Enghild<sup>1,2,\*</sup>

<sup>1</sup>Department of Molecular Biology and Genetics, Aarhus University, 8000 Aarhus, Denmark

<sup>2</sup>Interdisciplinary Nanoscience Center, Aarhus University, 8000 Aarhus, Denmark

<sup>3</sup>Biomedical Sciences Research Institute, Ulster University, Coleraine, Northern Ireland, BT52 1SA, UK

<sup>4</sup>Avellino Labs USA, Menlo Park, San Francisco, CA 94025, USA

\* To whom correspondence should be addressed: Jan J. Enghild, Department of Molecular Biology and Genetics, Aarhus University, Gustav Wieds vej 10C, 8000 Aarhus C., Denmark. Tel.: +45 87 15 54 49; E-mail: [jje@mb.au.dk](mailto:jje@mb.au.dk) and Tara Moore, Biomedical Sciences Research Institute, Ulster University, Cromore Road, Coleraine, Northern Ireland, BT52 1SA, UK. Tel: +44 28 7012 4577, E-mail: [tara.moore@ulster.ac.uk](mailto:tara.moore@ulster.ac.uk)

**Abbreviations:** ECM, extracellular matrix; GCD2, Granular corneal dystrophy type 2; LFQ, label-free quantification; TGFBIp, Transforming growth factor  $\beta$ -induced protein; WT, wild-type; DMSs, differently methylated sites

**Keywords:** Methylation, Cornea, Granular corneal dystrophy type 2, Label-free quantification, TGFBIp

**Total number of words: 2.515**

**Abstract**

**Purpose:** Mutations in the transforming growth factor  $\beta$ -induced protein (TGFBIp) are associated with *TGFBI*-linked corneal dystrophies, which manifests as protein deposits in the cornea. A total of 70 different disease-causing mutations have been reported so far including the common R124H substitution, which is associated with granular corneal dystrophy type 2 (GCD2). The disease mechanism of GCD2 is not known and the current treatments, such as corneal transplantation, only offer temporary relief due to the reoccurrence of deposits. In this study, we compared the corneal protein profiles of the three genotypes (wild-type (WT), heterozygotes, and homozygotes) of a GCD2 mouse model using label-free quantitative LC-MS/MS.

**Results:** The mice do not display any corneal protein deposits and the global protein expression between the three genotypes is highly similar. However, the expression of mutated TGFBIp is 41% of that of the WT protein.

**Conclusions and Clinical Relevance:** It is proposed that the lowered expression level of mutant TGFBI protein relative to WT protein is the direct cause of the missing development of corneal deposits in the mouse. The overall protein profiles of the corneas were not impacted by the reduced amount of TGFBIp. Altogether, this supports a partial reduction in mutated TGFBIp as a potential treatment strategy for GCD2.

Transforming growth factor  $\beta$ -induced protein (TGFBIp) is an extracellular matrix (ECM) protein that is highly abundant in the human cornea.<sup>[1]</sup> Mutations in TGFBIp are associated with corneal dystrophies where protein accumulation in the cornea leads to loss of normal vision. Granular corneal dystrophy type 2 (GCD2), also called Avellino corneal dystrophy, has a mixed phenotype of both amorphous and amyloid deposits, with amyloid deposits appearing in the more advanced stage of the disease. To date, 70 different mutations in TGFBIp have been reported in relation to corneal dystrophies, one of which is the common R124H mutation, which causes GCD2.<sup>[2]</sup> Patients that are homozygous for the R124H TGFBIp mutation usually develop corneal opacities in the first decade of life and have a more severe phenotype than heterozygous GCD2 patients, who experience onset of the disease later in life. The current treatments of *TGFBI*-linked corneal dystrophies include corneal transplantation and corneal ablation of the affected area. Unfortunately, these treatments only offer temporary relief and the protein deposits will reoccur.

The mechanisms responsible for the TGFBIp aggregation in the cornea of GCD2 patients are unknown. Animal models are useful in elucidating the pathogenesis and treatment strategies of diseases and one mouse model showing a *TGFBI*-related corneal dystrophy phenotype has so far been developed.<sup>[3]</sup> Human TGFBI cDNA with the R124H mutation was inserted into the first exon of the mouse TGFBI DNA generating the transgenic TGFBI<sup>R124H</sup> mouse model. In the original paper, the mice developed corneal opacities with total incidence rates of 0.0% in wild-type (WT), 19.4% in heterozygotes, and 45.0% in homozygotes.<sup>[3]</sup> The expression of TGFBI<sup>R124H</sup> was confirmed by RT-PCR and protein staining confirmed the presence of amorphous and amyloid deposits in the anterior stroma. The mouse model reflects the human cases of GCD2 by having a higher incidence of granular opacities in homozygotes than in heterozygotes and a higher incidence of opacities in aged mice.<sup>[3]</sup> However, the phenotype of the mouse model was not as severe as the human case.

We have previously performed proteomic profiling of normal and plaque corneal tissue from patients with GCD2 caused by the R124H mutation.<sup>[4, 5]</sup> These studies showed that the protein composition and relative protein abundance in the deposits differed from the control samples. Accumulation of intact or nearly full-length TGFBIp in the protein deposits and a slight difference in proteolytic processing were also observed.

In this study we analysed the proteome of R124H transgenic mouse corneas in an attempt to understand the disease mechanisms leading to the GCD2 phenotype. We compared the corneal proteome of three WT, heterozygous, and homozygous mice (Supporting Information 1), and analysed the corneal protein composition and relative amount of TGFBIp. All the mice studied had not developed corneal deposits.

Detailed method descriptions are found in Supporting Information 2. All work in mice described within was conducted under the Animals (Scientific Procedures) Act 1986, Section 5, through a project license granted to Professor Tara Moore by the Department of Health which specified a programme of work and authorized that programme, of specified regulated procedures to animals of specified descriptions at a specified place or specified places. The eyes of the mice used for proteome analysis were examined for corneal deposits using a surgical microscope. No corneal deposits were observed in any of the corneas, though mice within this age (43-57 weeks) were expected to have the following incidence of corneal opacity: 0.0 % in WT, 12.5 % in heterozygotes, and 42.9 % in homozygotes.<sup>[3]</sup> Additional, heterozygous and homozygous mice (n=10 per group) at the age from three months to two years were also examined and did not show any deposits. The left corneas were subjected to CNBr chemical cleavage followed by enzymatic trypsin digestion. The recovered peptides were analysed by LC-MS/MS using a Q Exactive Plus mass spectrometer (ThermoFisher Scientific). The MS data were searched and quantified using MaxQuant (version 1.6.5.0) performing label-free quantification (LFQ) based on minimum of two peptides from each protein and searched against the Uniprot mouse reference proteome (version

23\_09\_2019; 21960 sequences) supplemented with the human TGFBIp sequence (Uniprot accession number: Q15582) modified with the R124H substitution. The data were processed in Perseus (version 1.5.3.2) and protein identification was based on a 1 % FDR threshold. Proteins were only included for quantification if they were quantified in all three biological replicates of each genotype group. A total of 525 proteins were quantified in WT corneas, 544 in heterozygotes, and 508 in homozygotes (Table 1, Supporting Information 3 and 4) herof a total of 444 quantified in all three genotypes (Fig. 1A, Supporting Information 5).

The 25 most abundant proteins in each genotype were highly similar and did not reveal any major changes (Table 1). No significant regulated proteins apart from TGFBIp were found by student's t-test between WT and heterozygous/homozygous corneas (Supplemental Information 6). ECM proteins like collagens, keratocan, serum albumin, alpha-2-macroglobulin, lumican, and decorin were highly represented among the most abundant proteins (Table 1). Aldehyde dehydrogenase was also highly abundant and is known to constitute up to 40 % of the soluble protein in the mammalian corneal epithelium.<sup>[6]</sup> Transketolase is also known to be a major protein in the corneal epithelial cells and comprise 10 % of the soluble proteins in the adult mouse cornea.<sup>[7]</sup>

We confirmed expression of R124H TGFBIp in heterozygotes and homozygotes by detection of a peptide containing the R124H amino acid substitution (Fig. 1B). TGFBIp was found to be differentially expressed by ANOVA analysis, which was expected since the three genotypes have different combinations of the human and mouse protein. The razor peptides (peptide sequences not unique to one protein) between human R124H TGFBIp and mouse WT TGFBIp were assigned to the mouse accession number (P82198). In order to obtain the total amount of TGFBIp in the heterozygotes and homozygotes the LFQ intensity of human and mouse TGFBIp were added together. This resulted in TGFBIp being the 24<sup>th</sup> and 22<sup>th</sup> most abundant protein in heterozygotes and homozygotes respectively, both with a molar percentage of  $0.7 \pm 0.1$  (Table 1). In WT corneas TGFBIp ranked as the 16<sup>th</sup> most abundant protein with a molar percentage of  $1.0 \pm 0.0$ . The

difference in molar percentage led us to examine the amount of TGFBIp expression in the different genotypes further. Relative quantification based on the intensities of the shared razor peptides showed that the protein level of mutated TGFBIp was 41 % of that of the endogenous WT protein (Fig. 1C). The lower intensity of TGFBIp in homozygote compared to WT were also confirmed by 2DE on the right corneas (Supplemental Information 7). The disease mechanism of GCD has been linked to change in solubility and/or stability of the mutated protein.<sup>[8]</sup> This may cause TGFBIp to aggregate due to the high TGFBIp concentration in the cornea. The lower expression of the mutated protein observed in this study could, therefore, explain the lack of deposits in the TGFBI<sup>R124H</sup> corneas. In humans, TGFBIp is the second most abundant protein in the human cornea making up 1% of the epithelium, 17.6% of the stroma, and 36.8% of the endothelium and Descemets membrane.<sup>[1]</sup> We previously found the amount of TGFBIp in mouse cornea to be 10-fold lower than in humans, which is supported by the lower molar percentage in our results compared to the human corneal proteome.<sup>[9]</sup>

The disease mechanism of TGFBI-linked corneal dystrophies has in several studies been linked to altered stability and aberrant proteolytic processing of the disease-causing TGFBIp mutants.<sup>[4,8,10]</sup> We performed 2DE of the proteins in the right cornea of the different genotypes and subsequently immunoblotted against TGFBIp. The immunoblots showed a lower intensity of TGFBIp in the homozygote compared to WT, supporting the proteomics data. A high molecular weight cluster (Figure 2, HMw) together with a low molecular weight cluster (Figure 2, LMw 1) were observed in all genotypes. The heterozygote and the homozygote showed another low molecular weight cluster (Figure 2, LMw 2) indicating altered proteolytic processing in accordance with previous studies but could also be caused by a difference in the primary sequence of human and mouse TGFBIp.<sup>[4,5]</sup> Furthermore, the characteristic “zigzag” degradation pattern seen for human corneal TGFBIp appeared less pronounced in mice, and TGFBIp isoforms displayed a shift toward

a lower pI in mice than in human cornea.<sup>[11]</sup> This may be due to differential processing of TGFBIP between the two species, which is supported by the TGFBIR124C mouse model recently developed.<sup>[12]</sup>

In this study, we found the mutant expression in the TGFBIR<sup>124H</sup> mouse model to be 41 % of the WT protein. Based on previous reports we expected some of these mice to show deposits<sup>[3]</sup> and we suggest that the lack thereof is due to the low mutant TGFBIP amount. Quantitation of mutated TGFBIP was not addressed in the original paper characterizing the TGFBIR<sup>124H</sup> mice that developed deposits.<sup>[3]</sup> We assume equal expression level of mutant and WT TGFBIP in early generations of TGFBIR<sup>124H</sup> mice and suggest that several generations of breeding could have induced a lower expression due to genetic imprinting. Examination of methylation of the transgene promotor and flanking regions confirmed that they were differently methylated than the WT. Whether the differential methylation affects transcription is unknown. Furthermore, the knock-in construct does not contain introns, which can be a source of reduced transgene expression. The slow disease progression and mild severity originally reported for this mouse model compared to human GCD2 cases most likely reflects the generally lower TGFBIP protein level in mice compared to human cornea. Therefore, it is crucial for the generation of future *TGFBIP*-linked corneal dystrophy mouse models to increase TGFBIP expression level to obtain a reliable phenotype development of corneal dystrophies within the life span of the mouse.

This study shows reduced amount of mutant protein and absence of phenotype, suggesting reduction of mutated TGFBIP as a novel treatment strategy in humans. Some studies have addressed this approach by RNA interference in cell culture and hold great potential for further testing.<sup>[10]</sup> Another therapeutic approach to reduce the amount of TGFBIP is CRISPR/Cas9 gene editing. This method can be used for mutant allele specific gene editing in heterozygotes reducing the amount of mutant TGFBIP while allowing the WT TGFBIP to be unaffected. This approach holds great promise for a therapeutic approach to a number of the *TGFBIP*-linked corneal dystrophies and indeed



autosomal dominant disorders in general.<sup>[11]</sup> In the case of homozygotes it is necessary to reduce the expression of both mutant alleles. This study show that the protein profiles of the homozygotes, which had 41% reduction in TGFBIP amount compared to WT, did not change significantly. Furthermore, our previous studies showed only minor changes in the corneal structure of a *TGFBIR* knock-out mouse model <sup>[9]</sup>, altogether supporting corneal TGFBIP reduction as a mean to treat *TGFBIR*-linked corneal dystrophies, without major disturbance of corneal homeostasis.

The mass spectrometry proteomics data have been deposited to the ProteomeXchange Consortium via the PRIDE partner repository with the dataset identifier PXD012902

### **Acknowledgements**

The authors thank Dr. Shigeto Shimmura (Keio University School of Medicine) and Dr. Eung Kweon Kim (Yonsei University College of Medicine) for sharing of the TGFBIR124H mouse model. The project was supported by the VELUX Foundation (00014557), Danish Council for Independent Research—Medical Sciences (DFF-4004-00471), the Novo Nordisk Foundation (Bio-MS), and Dagmar Marshalls Fond.

### **Funding**

The project was supported by the VELUX Foundation (00014557), Danish Council for Independent Research – Medical Sciences (DFF-4004-00471), the Novo Nordisk Foundation (Bio-MS), and Dagmar Marshalls Fond.

The authors have declared no conflict of interest.

## References

- [1] T. F. Dyrland, E. T. Poulsen, C. Scavenius, C. L. Nikolajsen, I. B. Thogersen, H. Vorum, J. J. Enghild, *J Proteome Res* 2012, 11, 4231.
- [2] R. Garcia-Castellanos, N. S. Nielsen, K. Runager, I. B. Thogersen, M. V. Lukassen, E. T. Poulsen, T. Goulas, J. J. Enghild, F. X. Gomis-Ruth, *Structure* 2017, 25, 1740; R. Lakshminarayanan, S. S. Chaurasia, V. Anandalakshmi, S. M. Chai, E. Murugan, E. N. Vithana, R. W. Beuerman, J. S. Mehta, *Ocul Surf* 2014, 12, 234.
- [3] K. Yamazoe, S. Yoshida, M. Yasuda, S. Hatou, E. Inagaki, Y. Ogawa, K. Tsubota, S. Shimmura, *PLoS One* 2015, 10, e0133397.
- [4] H. Karring, K. Runager, I. B. Thogersen, G. K. Klintworth, P. Hojrup, J. J. Enghild, *Exp Eye Res* 2012, 96, 163.
- [5] E. T. Poulsen, N. S. Nielsen, M. M. Jensen, E. Nielsen, J. Hjortdal, E. K. Kim, J. J. Enghild, *Proteomics* 2016, 16, 539.
- [6] R. A. Cuthbertson, S. I. Tomarev, J. Piatigorsky, *Proc Natl Acad Sci U S A* 1992, 89, 4004.
- [7] C. M. Sax, W. T. Kays, C. Salamon, M. M. Chervenak, Y. S. Xu, J. Piatigorsky, *Cornea* 2000, 19, 833.
- [8] K. Runager, R. V. Basaiawmoit, T. Deva, M. Andreasen, Z. Valnickova, C. S. Sorensen, H. Karring, I. B. Thogersen, G. Christiansen, J. Underhaug, T. Kristensen, N. C. Nielsen, G. K. Klintworth, D. E. Otzen, J. J. Enghild, *J Biol Chem* 2011, 286, 4951; M. Stenvang, N. P. Schafer, K. G. Malmos, A. W. Perez, O. Niembro, P. Sormanni, R. V. Basaiawmoit, G. Christiansen, M. Andreasen, D. E. Otzen, *J Mol Biol* 2018, 430, 1116.
- [9] E. T. Poulsen, K. Runager, N. S. Nielsen, M. V. Lukassen, K. Thomsen, P. Snider, O. Simmons, H. Vorum, S. J. Conway, J. J. Enghild, *FEBS J* 2018, 285, 101.
- [10] a) K. E. Han, S. I. Choi, W. S. Chung, S. H. Jung, N. Katsanis, T. I. Kim, E. K. Kim, *Mol. Vision* 2012, 18, 1755; b) D. G. Courtney, E. T. Poulsen, S. Kennedy, J. E. Moore, S. D. Atkinson, E. Maurizi, M. A. Nesbit, C. B. Moore, J. J. Enghild, *Invest. Ophthalmol. Visual Sci.* 2015, 56, 4653.
- [11] E. T. Poulsen, N. S. Nielsen, C. Scavenius, E. H. Mogensen, M. W. Risor, K. Runager, M. V. Lukassen, C. B. Rasmussen, G. Christiansen, M. Richner, H. Vorum, J. J. Enghild, *J. Biol. Chem.* 2019, 294, 11817.
- [12] a) N. S. Nielsen, E. T. Poulsen, M. V. Lukassen, C. Chao Shern, E. H. Mogensen, C. E. Weberskov, L. DeDionisio, L. Schauser, T. C. B. Moore, D. E. Otzen, J. Hjortdal, J. J. Enghild, *Prog. Retinal Eye Res.* 2020, 100843; b) K. Kitamoto, Y. Taketani, W. Fujii, A. Inamochi, T. Toyono, T. Miyai, S. Yamagami, M. Kuroda, T. Usui, Y. Ouchi, *Sci. Rep.* 2020, 10, 2000.
- [13] B. G. Poulson, K. Szczepski, J. I. Lachowicz, L. Jaremko, A. H. Emwas, M. Jaremko, *RSC Adv.* 2020, 10, 215.
- [14] a) D. G. Courtney, S. D. Atkinson, J. E. Moore, E. Maurizi, C. Serafini, G. Pellegrini, G. C. Black, F. D. Manson, G. H. Yam, C. J. Macewen, E. H. Allen, W. H. McLean, C. B. Moore, *Invest Ophthalmol Vis Sci* 2014, 55, 977; b) V. S. Yellore, S. A. Rayner, A. J. Aldave, *Invest Ophthalmol Vis Sci* 2011, 52, 757; C. Yuan, E. J. Zins, A. F. Clark, A. J. Huang, *Mol Vis* 2007, 13, 2083.
- [15] a) D. G. Courtney, J. E. Moore, S. D. Atkinson, E. Maurizi, E. H. Allen, D. M. Pedrioli, W. H. McLean, M. A. Nesbit, C. B. Moore, *Gene Ther* 2016, 23, 108; b) K. A. Christie, D. G. Courtney, L. A. DeDionisio, C. C. Shern, S. De Majumdar, L. C.

Mairs, M. A. Nesbit, C. B. T. Moore, Sci Rep 2017, 7, 16174; c) C. B. T. Moore, K. A. Christie, J. Marshall, M. A. Nesbit, Prog Retin Eye Res 2018, 65, 147.

**Figure legends**

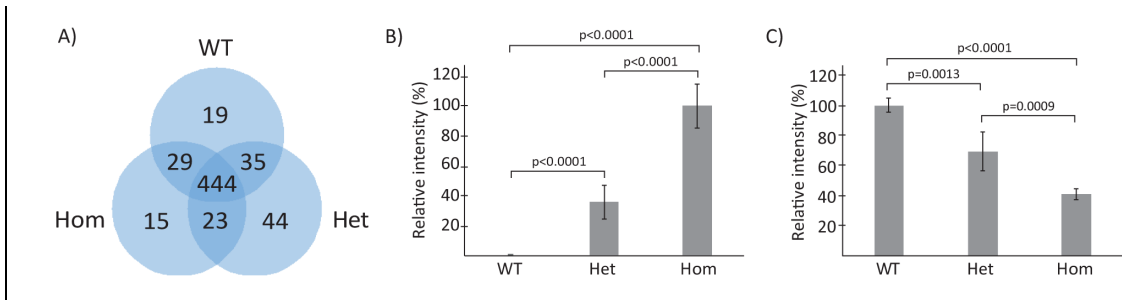
**Figure 1.** Venn diagram of expressed proteins and TGFBIp expression in the three genotypes. A) Venn diagram of the number of proteins quantified in WT, heterozygous (Het), and homozygous (Hom) TGFBI<sup>R124H</sup> mouse corneas. Full list of sorted accession numbers can be found in Supporting Information 5. B) Relative quantification of the human peptide containing the R124H mutation. C) Quantification of relative TGFBIp amount in the three genotypes based on intensity of razor peptides between the mouse and human sequence (n = 3 per genotype). The t-test p-values are indicated.

**Figure 2.** 2DE immunoblots of TGFBIp in WT, heterozygous (Het), and homozygous (Hom) TGFBI<sup>R124H</sup> mouse corneas. The TGFBIp amount in the homozygote is lower than the WT and heterozygote and no accumulation of full-length (FL) protein in the homozygote was observed. A high and low molecular weight (HMw, LMw 1) cluster of proteolytic processed TGFBIp were present in all samples. Further degradation represented by another LMW cluster (LMw 2) was seen in the homozygous and the heterozygous sample.

**Table 1.** Molar percentage of the 20 most abundant proteins in WT, Heterozygous, and Homozygous TGFB1<sup>R124H</sup> mice corneas

WT			Heterozygote			Homozygote					
No.	Accession	Protein name	Molar %	No.	Accession	Protein name	Molar%	No.	Accession	Protein name	Molar%
1	P11087	Collagen alpha-1 (I) chain	17.9 ± 0.3	1	P11087	Collagen alpha-1 (I) chain	18.3 ± 2.5	1	P11087	Collagen alpha-1 (I) chain	19.7 ± 0.1
2	Q01149	Collagen alpha-2 (I) chain	14.3 ± 0.3	2	Q01149	Collagen alpha-2 (I) chain	13.8 ± 2.1	2	Q01149	Collagen alpha-2 (I) chain	15.6 ± 0.4
3	E9PWQ3	Collagen alpha-3 (VI) chain	9.7 ± 0.4	3	E9PWQ3	Collagen alpha-3 (VI) chain	8.8 ± 1.1	3	E9PWQ3	Collagen alpha-3 (VI) chain	9.5 ± 0.5
4	Q922U2	Keratin, type II cytoskeletal 5	4.0 ± 0.1	4	Q922U2	Keratin, type II cytoskeletal 5	3.4 ± 0.4	4	Q60847	Collagen alpha-1 (XII) chain	3.5 ± 0.4
5	Q60847	Collagen alpha-1 (XII) chain	3.6 ± 0.2	5	Q47739	Aldehyde dehydrogenase	3.3 ± 0.1	5	Q922U2	Keratin, type II cytoskeletal 5	3.4 ± 0.2
6	Q47739	Aldehyde dehydrogenase	3.5 ± 0.1	6	P40142	Transketolase	3.1 ± 0.1	6	Q47739	Aldehyde dehydrogenase	3.1 ± 0.1
7	P40142	Transketolase	3.5 ± 0.2	7	Q60847	Collagen alpha-1 (XII) chain	3.1 ± 0.4	7	Q02788	Collagen alpha-2 (VI) chain	3.0 ± 0.2
8	Q64291	Keratin, type I cytoskeletal 12	3.2 ± 0.1	8	Q02788	Collagen alpha-2 (VI) chain	2.9 ± 0.4	8	P40142	Transketolase	3.0 ± 0.3
9	Q02788	Collagen alpha-2 (VI) chain	3.1 ± 0.1	9	Q64291	Keratin, type I cytoskeletal 12	2.8 ± 0.4	9	Q04857	Collagen alpha-1 (VI) chain	2.9 ± 0.2
10	Q04857	Collagen alpha-1 (VI) chain	2.9 ± 0.1	10	Q04857	Collagen alpha-1 (VI) chain	2.7 ± 0.3	10	Q64291	Keratin, type I cytoskeletal 12	2.8 ± 0.2
11	Q6GQT1	Alpha-2-macroglobulin-P	1.8 ± 0.1	11	P24622	Alpha-crystallin A	2.1 ± 2.8	11	Q6GQT1	Alpha-2-macroglobulin-P	1.6 ± 0.3
12	O35367	Keratocan	1.7 ± 0.0	12	O35367	Keratocan	1.6 ± 0.2	12	O35367	Keratocan	1.6 ± 0.1
13	113P63260	Actin, cytoplasmic 2	1.7 ± 0.1	13	Q6GQT1	Alpha-2-macroglobulin-P	1.6 ± 0.1	13	P63260	Actin, cytoplasmic 2	1.5 ± 0.1
14	P07724	Serum albumin	1.5 ± 0.1	14	P63260	Actin, cytoplasmic 2	1.6 ± 0.0	14	P07724	Serum albumin	1.3 ± 0.1
15	Q8CGP2	Histone H2B	1.1 ± 0.0	15	P07724	Serum albumin	1.5 ± 0.2	15	Q8CGP2	Histone H2B	1.1 ± 0.1
16	P82198	TGFB1p	1.0 ± 0.0	16	P23927	Alpha-crystallin B	1.1 ± 1.4	16	P51885	Lumican	0.9 ± 0.1
17	O88207	Collagen alpha-1 (V) chain	1.0 ± 0.0	17	Q8CGP2	Histone H2B	1.0 ± 0.0	17	O88207	Collagen alpha-1 (V) chain	0.9 ± 0.2
18	P51885	Lumican	0.9 ± 0.0	18	O88207	Collagen alpha-1 (V) chain	1.0 ± 0.2	18	P62806	Histone H4	0.8 ± 0.0
19	P62806	Histone H4	0.9 ± 0.0	19	P51885	Lumican	0.9 ± 0.1	19	P02463	Collagen alpha-1 (IV) chain	0.8 ± 0.7
20	P28654	Decorin	0.8 ± 0.0	20	P02463	Collagen alpha-1 (IV) chain	0.8 ± 0.8	20	P28654	Decorin	0.7 ± 0.1
21	Q3U962	Collagen alpha-2 (V) chain	0.7 ± 0.0	21	P62806	Histone H4	0.8 ± 0.0	21	P82198	Collagen alpha-2 (IV) chain	0.7 ± 0.7
22	Q62000	Mimecan	0.7 ± 0.0	22	P62696	Beta-crystallin B2	0.8 ± 1.0	22	P82198+ Q15582	TGFB1p	0.7 ± 0.1
23	Q61414	Keratin, type II cytoskeletal 15	0.6 ± 0.1	23	P82198	Collagen alpha-2 (IV) chain	0.8 ± 0.7	23	Q3U962	Collagen alpha-2 (V) chain	0.6 ± 0.1
24	O09131	Glutathione S-transferase	0.6 ± 0.0	24	P82198 + Q15582	TGFB1p	0.7 ± 0.1	24	Q61414	Keratin, type II cytoskeletal 15	0.6 ± 0.2
25	P84228	Histone H3.2	0.5 ± 0.0	25	Q3U962	Collagen alpha-2 (V) chain	0.7 ± 0.1	25	Q62000	Mimecan	0.6 ± 0.1

The molar percentage was calculated by dividing the LFQ intensity for a given protein by the total LFQ intensity for all proteins in a given sample. Proteins were included if quantified in all three biological replicates in one group.

**Figure 1****Figure 2**